INJECTOR LAYOUT OPTIMIZATION FOR THE PHASE-I STAGE OF THE SPring-8 COMPACT SASE SOURCE (SCSS) PROJECT

Yujong Kim*, T. Shintake, K. Togawa, H. Matsumoto, and H. Kitamura, RIKEN, SPring-8, Japan
K. Sawada, Sumitomo Heavy Industries Ltd, Japan
Klaus Flöttmann, DESY, Germany

Abstract

At the Phase-I stage of the SPring-8 Compact SASE Source (SCSS) project, the injector should supply the high quality beam with 125 A or higher peak current and 1.4 μm or lower projected normalized rms emittance to operate the bunch compressor properly and to saturate the SASE-FEL within 13.5 m long undulator. In this paper, we have described the injector optimization process to supply the required high quality beam at the Phase-I stage of the SCSS project.

1 INTRODUCTION

In April 2001, the SCSS project was launched to generate the fourth generation light source with the linac-based SASE-FEL technology [1]. During the Phase-I stage (2001-2005), the injector, one C-band main linac, one bunch compressor, and one in-vacuum undulator will be installed to generate 40 nm wavelength radiation with 230 MeV electron beam [1]-[3]. The SCSS injector consists of the 500 kV pulse-gun with the CeB_6 single crystal cathode, 476 MHz buncher and booster cavities, and finally, 1428 MHz L-band standing wave linac with the alternating period structure (APS) [1]-[4]. For the high stability and easy tuning, we chose the pulse-gun instead of the RF-gun [1]. The full description on the pulse-gun can be found in the reference [1] and [4]. In this paper, we will describe the injector optimization process to supply the required high quality beam at the Phase-I stage of the SCSS project.

2 OPTIMIZATION CONCEPTS

The current optimized injector layout and design beam parameters for the Phase-I stage are shown in Fig. 1 where E is the beam energy, σ_δ is the projected rms relative energy spread, $\Delta\tau$ is the full width bunch length, I_{pk} is the peak current, Q is the single bunch charge, and ϵ_n is the projected transverse normalized rms emittance. By operating the CeB_6 single crystal cathode at $1450°$C, and by applying 500 kV pulse voltage at 50 mm cathode-anode gap, 0.5 MeV, 3 A, 1.5 μs (FW) long pulse with 300 ns flat-top will be extracted from the cathode. Since the cathode radius is 1.5 mm, the normalized thermal rms emittance is about 0.4 μm. And at the exit of gun, the total projected normalized rms emittance is also close to 0.4 μm because the space charge induced emittance dilution at the gap is small enough under 10 MV/m accelerating gradient and 3 A beam current conditions [1], [4].

For the transverse beam focusing, we will use the 25 mm short double Einzel lens over all injector layout to align easily and to compensate the beam rotation [1]. At the downstream of the pulse-gun, the 1.5 μs long pulse with 300 ns flat-top will be reduced to 2.1 ns (FW) by the beam deflector which the high-voltage pulse gates the beam [5].

After the beam deflector, the 2.1 ns long pulse will be focused by the Einzel lens again. Then the pulse will be sent to the buncher where the energy of electron will be modulated with 400 kV peak-to-peak amplitude as shown in Fig. 1. Since electrons are non-relativistic, the energy modulation gives rise to the velocity modulation for the drifting bunching. When the non-relativistic electron beam goes through a single cell RF cavity, the electron phase on RF fields will be changed by the time-dependent fringe fields at the cavity entrance and exit regions. The projected emittance dilution due to the fringe fields is given by

$$\Delta\epsilon_n = \frac{\pi r^2}{2}\frac{E_{gain}}{m_e c^2}\frac{1}{\beta^2\gamma^2\lambda_{RF}}\frac{\Delta\phi^2}{8}, \qquad (1)$$

where r is the beam radius, E_{gain} is the energy gain of the RF cavity, $m_e c^2$ the electron rest mass energy, β is the relativistic velocity, γ is the Lorentz factor, λ_{RF} is the RF wavelength, and $\Delta\phi$ is the bunch length in radian [6]. This emittance dilution can be reduced by choosing the low RF frequency of the cavity, by adjusting the energy gain at those regions, and by keeping small beam size and short bunch length at those regions [1], [6]. After considering the commercially available klystron, we have chosen 476 MHz for the RF frequencies of the buncher and booster cavities and 1428 MHz for that of the standing wave linac [1].

At the drift space between the buncher and the booster, where the bunch length is compressed by the combined action of the buncher and the drift space, the space charge force becomes strong if the bunch charge is high. The space charge force and the emittance dilution in the drift space can be controlled by chopping and energy-filtering the electron beam right after the buncher. Then, the electron beam is strongly focused by the Einzel lens to keep the beam size within 3 mm until the booster as shown in Fig. 1. By the help of the chopping and energy-filtering, we can select the only high quality beam with $\Delta\tau \sim 333$ ps, $Q \sim 1$ nC, and $\epsilon_n \sim 0.5$ μm as shown in Figs. 1 and 2 [7]. In Fig. 2, each ellipse area means the slice normalized rms emittance ϵ_{ns}, and the projected normalized rms emittance of 0.5 μm is close to the average slice normalized rms emittance of 0.42 μm because all ten ellipsis are well-aligned.

* yjkim@spring8.or.jp, http://www-xfel.spring8.or.jp

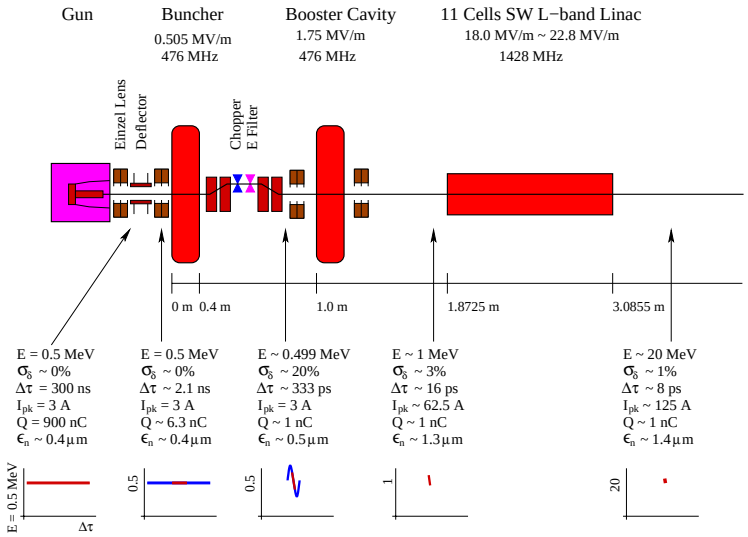

Figure 1: Optimized injector layout and design beam parameters for the Phase-I stage of the SCSS project.

According to the estimation result, where the space charge force is ignored, about 1.5 m long drift space after the buncher is required to compress the bunch length from 333 ps to 8 ps [6]. However the space charge force becomes strong before the beam goes through 1.5 m downstream as the bunch length is compressed. The transverse beam spreading due to the space charge force is given by

$$\frac{d^2r}{ds^2} = \frac{eE_r}{m_e c^2}\frac{1}{(\beta\gamma)^3} = \frac{e}{m_e c^2}\frac{I_{pk}}{2\pi\epsilon_0 rc}\frac{1}{(\beta\gamma)^3}, \qquad (2)$$

where E_r is the radial electric field [6]. Therefore the beam spreading due to the space charge force can be reduced to about four times smaller by increasing the beam energy to 1 MeV at the booster [1], [6].

Right after booster, we have applied the strong focusing by the Einzel lens to keep the beam size within 1.5 mm at the entrance of the L-band linac, which will help in reducing the emittance dilution due to the fringe field of the L-band linac [8]. After drifting 0.4725 m long space from the booster, the electron beam is compressed further. Our standing wave linac consists of $\pi/2$ mode eleven cells. The accelerating gradient of the middle cells is about 22.8 MV/m while those at the entrance and exit of the L-band linac are reduced to 18 MV/m to control the emittance dilution due to the fringe field [6], [8]. Inside of the standing wave linac, the transverse beam size can be effectively reduced by the second order ponderomotive focusing force in the standing wave linac [8].

3 SIMULATION RESULTS

To understand the slice and projected emittance dilution along the injector, we have invested the effective radial field component $(\vec{E} + \vec{v} \times \vec{B})_r$ due to the space charge with ASTRA code as shown in Fig. 3. Right after chopping and energy-filtering, the effective radial component is well-linear along the beam radius r, and it is also independent

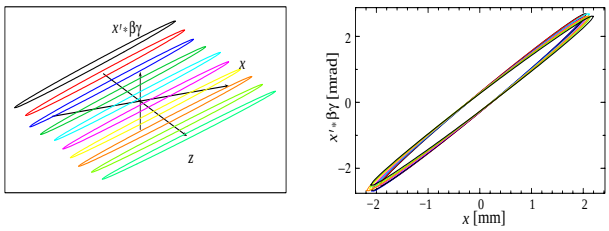

Figure 2: ASTRA simulation results right after chopping and energy-filtering for $E \simeq 0.5$ MeV, $Q \simeq 0.92$ nC, $\Delta\tau \simeq 250$ ps (FW), and the rms beam size $\sigma_{x,y} \simeq 2$ mm: (left) the transverse phase space distribution for ten slices along the bunch, (right) the transverse phase space distribution when the viewpoint is on the z-axis.

of the longitudinal deviation dz as shown in Fig. 3(left). In this case, the geometric slice emittance will be small because the radial divergence r' will be linearly changed along the beam radius r, and the projected emittance is also small because the effective radial component is independent of the longitudinal deviation dz, and ellipsis of the slice emittances are well-aligned as shown in Fig. 2 [9]. After the drifting bunching, the charge distribution along bunch is not uniform due to the sinusoidal RF curvatures at the buncher, the booster, and the L-band linac. In this case, though the beam energy is high enough, and the magnitude of the space charge force is reduced, the nonlinearity in the space charge force becomes strong. Therefore, the effective radial component is nonlinear along the beam radius, and it is also dependent on the longitudinal deviation dz as shown in Fig. 3(right). Here the geometric slice emittance is increased because the radial divergence r' is nonlinearly changed along the beam radius r, and the projected emittance is also increased because ellipsis of the slice emittances are rotated or misaligned according to their longitudinal deviation dz.

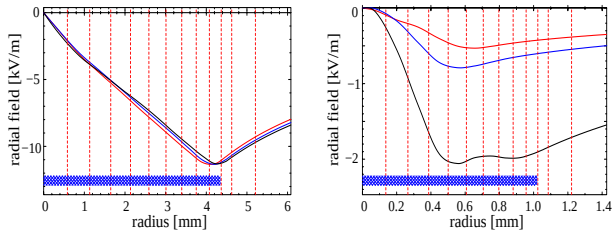

Figure 3: ASTRA simulation results of the effective radial field component $(\vec{E} + \vec{v} \times \vec{B})_r$ of the space charge field: (left) right after energy-filtering, (right) at the end region of the L-band linac. Here red, blue, and black lines mean the effective radial field at $dz = -\sigma_z$, $dz = 0$, and $dz = \sigma_z$, respectively, and the blue bar means the radial beam size.

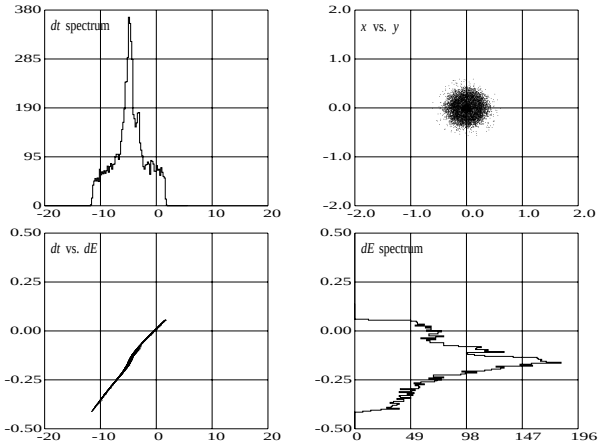

Figure 4: PARMELA simulation results at the end of the injector: (upper left) longitudinal time deviation dt [ps] versus particle number, (upper right) transverse beam profile, x [mm] versus y [mm], (lower left) longitudinal phase space distribution, dt [ps] versus dE [MeV], and (lower right) particle number versus energy deviation dE [MeV].

We have compensated the emittance dilution due to the nonlinearity in the space charge force by optimizing the chopping and energy filtering conditions, and the RF phases in the buncher, booster, and the L-band linac. The current optimized PARMELA simulation results after the SCSS injector are shown in Fig. 4. Here the longitudinal phase space distribution has good linearity along the bunch length, and the beam is well-focused by the second order ponderomotive focusing force in the standing wave linac. Since dt and dE spectra are a kind of the Lorentzian distribution due to the strong drift bunching, we are trying to modify that to the uniform distribution against the coherent synchrotron radiation in the bunch compressor and the longitudinal wakefield in the C-band linacs.

The current optimized beam parameters after the SCSS injector is summarized in Table 1 where the simulation-confirmed beam parameters at the ends of the gun and the injector are summarized in the first and the second columns, and the design beam parameters at the end of the injector are summarized in L-band* column. Since electrons being apart further than one cooperation length ($\sim \mu$m) will not interact with each other, we should focus the slice parameters to predict FEL performance [3]. The current optimized emittance and energy spread are much small than our design values while the peak current (bunch length) and the single bunch charge are lower (longer) than our design values. We expect that those unconfirmed parameters can be obtained by optimizing chopping and energy filtering conditions, by adjusting the drift space and the RF phase of booster for the drift bunching, by optimizing the beam energy of booster to control the space charge force, and by optimizing the L-band linac for the RF compressing [10].

Table 1: Injector parameters of the SCSS Phase-I stage.

Parameter	Gun	L-band	L-band*
beam energy E, MeV	0.5	20.6	> 20
slice emittance ϵ_{ns}, μm	0.4	0.7	< 1.4
projected emittance ϵ_n, μm	0.4	0.9	< 1.4
slice energy spread $\sigma_{\delta s}$, %	0.0	0.03	< 0.05
projected energy spread σ_δ, %	0.0	0.53	< 1.0
single bunch charge Q, nC	900	0.92	> 1.0
bunch length $\Delta\tau$ (FW), ps	3×10^5	13	< 8.0
bunch length Δz (FW), mm	·	3.9	< 2.4
peak current I_{pk}, A	3.0	71	> 125

4 SUMMARY

According to the current optimized results, our injector will generate the high quality beam with $\epsilon_n \simeq 0.9$ μm, $Q \simeq 0.92$ nC, and $\Delta\tau \simeq 13$ ps (FW) at about 20 MeV. Although the design bunch length of 8 ps (FW) is not confirmed yet, we expect that the bunch length will be obtained by optimizing the injector layout further. Now we are under optimizing the new injector layout with two traveling wave L-band linacs to reduce the bunch length to 4 ps.

5 REFERENCES

[1] T. Shintake *et al.*, in *Proc. SPIE2001*, San Diego, USA, 2001; http://www-xfel.spring8.or.jp.

[2] Yujong Kim *et al.*, in *Proc. EPAC2002*, Paris, France, 2002.

[3] Yujong Kim *et al.*, in these proceedings; Yujong Kim *et al.*, in *Proc. 24th ICFA workshop*, Hyogo, Japan, to be published; http://www-xfel.spring8.or.jp.

[4] K. Togawa *et al.*, in *Proc. 24th ICFA workshop*, Hyogo, Japan, to be published; http://www-xfel.spring8.or.jp.

[5] T. Kobayashi *et al.*, in *Proc. EPAC2002*, Paris, France, 2002.

[6] A. Wu Chao and M. Tigner, *Handbook of Accelerator Physics and Engineering*, (World Scientific, Singapore, 1998), pp. 99-103.

[7] http://www.desy.de/∼mpyflo/Astra_dokumentation/.

[8] J. Rosenzweig and L. Serafini, Phys. Rev. E **49**, 1599 (1994).

[9] M. Krassilnikov *et al.*, in *Proc. PAC2001*, Chicago, USA, 2001.

[10] L. Serafini *et al.*, in *Proc. PAC2001*, Chicago, USA, 2001.